Ettringite as a factor causing structural strengthening of fluvial sand from the Praski terrace (Warsaw, Poland)

PIOTR ZAWRZYKRAJ[1], PAWEŁ RYDELEK[2], ANNA BĄKOWSKA[2*] and KRZYSZTOF CABALSKI[2]

[1] *University of Warsaw, Faculty of Geology, Department of Engineering Geology and Geomechanics,
Żwirki i Wigury 93, 02-089 Warszawa, Poland; e-mail: Piotr.Zawrzykraj@uw.edu.pl*
[2] *University of Warsaw, Faculty of Geology, Department of Environmental Protection and Natural Resources,
Żwirki i Wigury 93, 02-089 Warszawa, Poland;
e-mails: Pawel.Rydelek@uw.edu.pl, anna.bakowska@uw.edu.pl, krzysztof.cabalski@uw.edu.pl*
* Corresponding author

ABSTRACT:

Zawrzykraj, P., Rydelek., P., Bąkowska, A. and Cabalski, K. 2022. Ettringite as a factor causing structural strengthening of fluvial sand from the Praski terrace (Warsaw, Poland). *Acta Geologica Polonica*, **72** (4), 519–528. Warszawa.

Engineering activity may lead to uncontrolled changes in the geological environment. This paper presents an example of structural changes in fluvial sand of the Praski terrace (in Warsaw) caused by the activity of a temporary concrete batching plant. Our investigations made it possible to identify the material responsible for the structural anomalies observed in the bottom of the trench excavation. The compound responsible for the cementation phenomenon was identified as ettringite – hydrated calcium aluminosulphate: $Ca_6Al_2[(OH)_{12}(SO_4)_3]\cdot 26H_2O$. The source of ettringite were most probably significant volumes of contaminants coming from the temporary concrete batching plant (e.g., from the rinsing of concrete mixers and/or installations for concrete storage and transportation). While penetrating into the ground, ettringite caused extensive cementation of the soil mass, mainly in the saturation zone. As a result, the mineral (chemical) composition of the inter-grain space changed and the structure of the sand was strengthened. The estimated zone of volumetric changes in soil properties was about 6 thousand m^3. However, analysis of the chemical composition of groundwater for its potential sulphate contamination, did not reveal any anomalous concentrations of sulphates.

Key words: Praski terrace; Anthropogenic soils; Ettringite; Cementation; Contamination.

INTRODUCTION

Geological investigations in urban areas mainly focus on engineering geological, hydrogeological, and geochemical issues, and on the identification of geohazards (Kong and Komoo 1990; Radzikowski *et al.* 2017). These investigations are also often linked to analysis of the impact of human activities on the soil and groundwater environment (Culshaw and Price 2011; Kowalczyk *et al.* 2017), as engineering activities may cause changes in the geological environment, e.g., uncontrolled volume changes of expansive

soil (Kumor 2016), additional settlement due to the dewatering system (Dobak and Chylińska 2007), or increase of regional seismicity and landslide hazards due to dam construction (Tang *et al.* 2019). Also, the co-occurrence of natural and anthropogenic soils requires precise determination of the extent of each soil type and very often causes difficulties in the analysis of engineering geological conditions (Bażyński *et al.* 1999).

In this paper, we analysed an interesting case of structural changes in river sand. During routine geological investigation carried out just before the
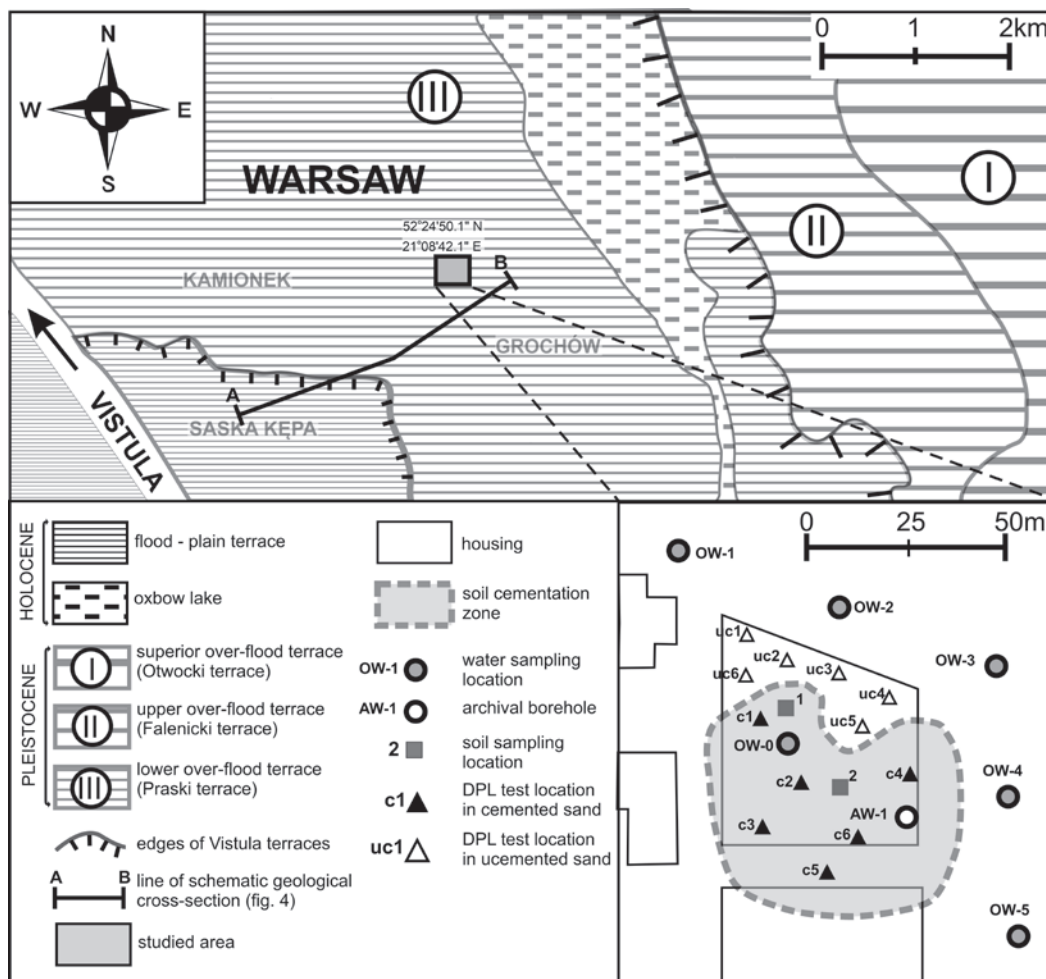
Text-fig. 1. Location of the study area on the Vistula terraces.

formation of the bottom slab, we found an extensive zone of strengthened (cemented) river sand at the bottom of a trench excavation. We noted a clear change of the typical colour from yellow and yellow-grey to light grey. We observed a brittle failure mechanism during excavation by construction machines. Also, we documented a significant soil resistance to sounding and drilling, much higher than typical for similar soil. These field observations led us to investigate the causes of these anomalies under laboratory conditions.

Location

The study area is located in Warsaw in a dense residential area (Text-fig. 1). In terms of geomorphological conditions, the area is located within the lower over-flood terrace called "the Praski terrace" (Sarnacka 1992). The terrace surface is located at
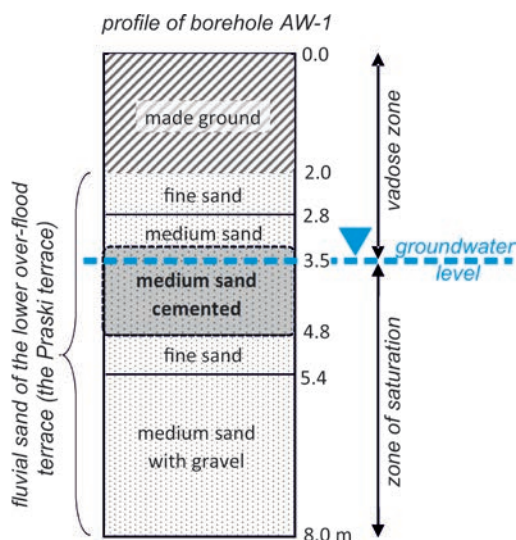
Text-fig. 2. AW-1 borehole log (location of the borehole presented in Fig. 1).
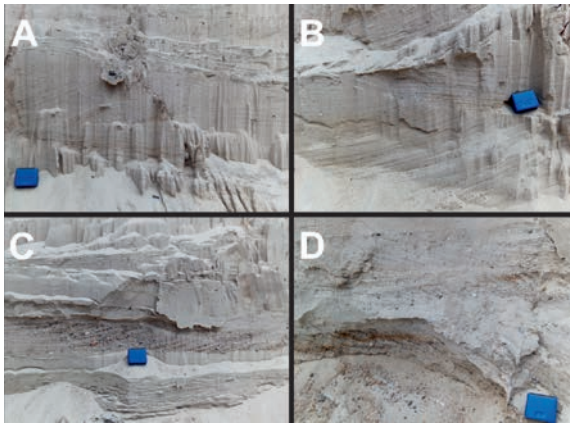
Text-fig. 3. Pictures of natural fluvial sand taken in the excavation wall near point uc3 (as located in Fig.1) A. Cross-stratified medium sand. Depth approximately 2.5 m. B. Cross-stratified medium sand with gravel. Depth approx. 2.5 m. C. Cross-stratified medium sand and coarse sand with gravel and adjacent fine sand. Depth approximately 3.0 m. D. Cross-stratified coarse sand with gravel. Depth approx. 3.0 m. Width of blue marker – 7 cm.

an elevation of 82.5–87.5 m above sea level (5–10 m above the level of the Vistula river). The Praski over-flood terrace is 2–3 m higher than the flood-plain terrace.

The geological profile starts with fluvial soil of the North-Polish glaciation (the Bölling interphase, Sarnacka 1992). It is mainly medium sand and coarse sand, locally changing into fine sand. The grain size increases gradually with depth (Text-figs 2 and 3).

The thickness of fluvial sand reaches approx. 8–12 m (Sarnacka 1992). Underneath, there is sandy and gravelly sediment of the Eemian interglacial of similar thickness. Further down, there is Neogene clay (variegated clays). The groundwater table is sta-bilised at a depth of 3.5–4.0 m (Text-figs 2 and 4).

MATERIALS AND METHODS

The mechanical properties of the sand were characterised directly under in situ conditions. DPL (Dynamic Probing Light) tests were used to deter-mine the mechanical effect of uncontrolled cementa-tion in fluvial sand. This is a standardised test (ISO 22476-2:2005) commonly used to assess the com-paction of non-cohesive soils. During the test, the penetration blow counts needed to immerse the cone tip for every 10 cm of probe penetration were docu-mented. The direct result of the measurements is a graph of penetration resistance, which is an indicator of the mechanical properties of non-cohesive soils.

Soil samples for laboratory testing were collected from the bottom of the trench excavation at a depth of approximately 4.0 m in June 2018. All laboratory tests were performed in the facilities of the Faculty of Geology at the University of Warsaw.

Five groundwater samples were also collected. The content of sulphate ions was determined for all groundwater samples by the spectrophotometric method with the use of Hach apparatus. In addition, for one sample (OW-0, collected from the bottom of the trench, Text-fig. 1) we determined the content of several cations: Ca, Mg, K, Na, Al, Ba, Cd, Co, Cr, Cu, Fe, Mn, Ni, Pb, Sr, Ti, V, Zn. ICP-OES Optima
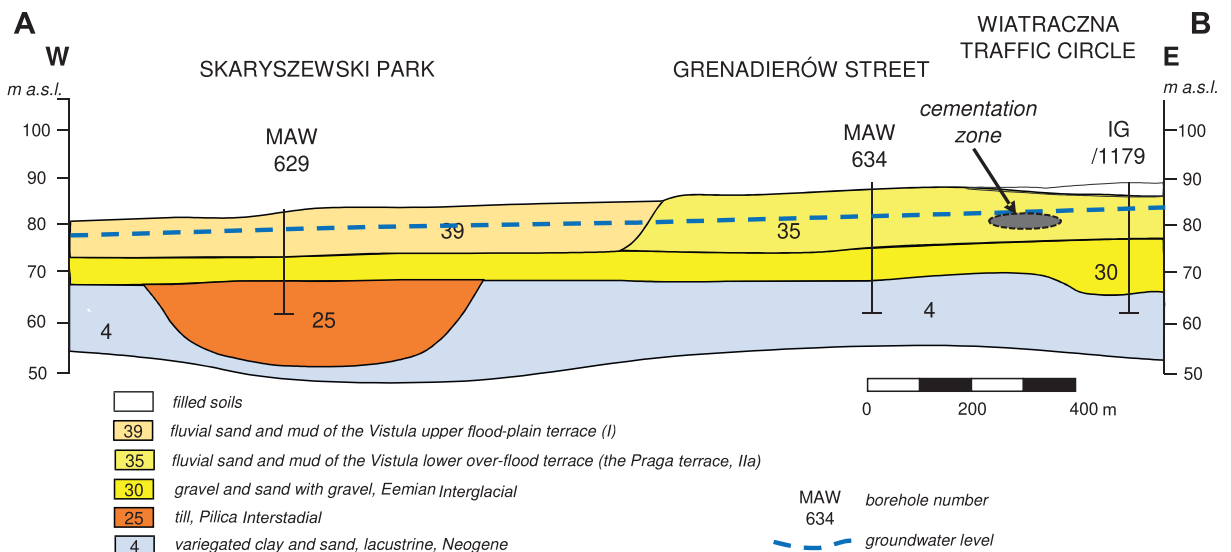
Text-fig. 4. Schematic geological cross-section of studied area (after Sarnacka 1992, modified).

5300 DV spectrometer (by Perkin-Elmer) was used for cation analysis. The pH was determined by the electrometric method (Head 1992).

SEM pictures were obtained using a JSM-6380LA scanning electron microscope coupled to a JEOL EDS electron microprobe.

XRD studies were performed at the Laboratory of Electron Microscopy, Microanalysis and X-ray Diffraction using an X'Pert PRO MPD powder X-ray diffractometer (PANalytical B.V. – Netherlands) using the Bragg-Brentano method. The results were analysed using X'Pert HighScore Plus software (ver. 2.2e).

The carbonate content was determined by Scheibler's method (BS EN ISO 10693:2014).

RESULTS

During fieldwork in June 2018 unusual soil changes were observed at the bottom of the trench excavation (Text-fig. 5). These changes were manifested in a macroscopically visible colour change and cementation of fluvial sand (Text-figs 6, 7).

Sieve analysis of a representative soil sample
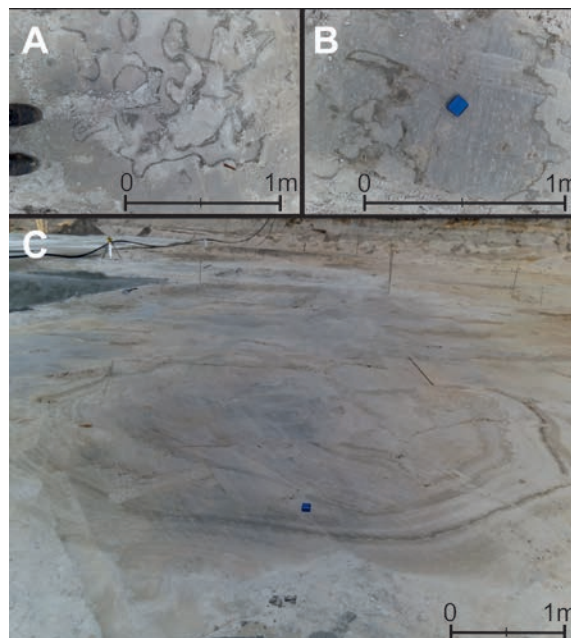
Text-fig. 5. Spherical structures formed as a result of seepage of the contaminant front. Colour change is visible in the zone of structural changes. Pictures taken at: A – point c5, B – point c6, C – point OW-0 (as located in Text-fig. 1).

Text-fig. 6. Unnatural grey colour of cemented fluvial sand (originally yellow in colour) forming blocks and crumbs during mining. Picture taken at point c4 (as located in Text-fig. 1).

Text-fig. 7. Samples of cemented fluvial sand collected for laboratory tests (air-dry condition).

(Text-fig. 8) allowed quantitative grain size analysis and soil classification. According to the Unified Soil Classification System (ASTM D2487-11) it is a poorly graded sand SP. According to the European Standard ISO 14688-2:2017 it is medium sand mSa, gap graded. The coefficient of permeability k calculated on the basis of effective diameter d_{20} (USBSC formula k = 0.0036 $d_{20}^{2,3}$ m/s) is equal to 1.93×10^{-4} m/s. This is a high value, indicating well-permeable soil (Pazdro and Kozerski 1990).

A quantitative evaluation of the spatial extent of the structural changes in the contour of the trench excavation was carried out. The area affected by the uncontrolled strengthening was approximately 2500 m^2 (Text-fig. 1), taking into account also a fragment of the building foundation in the southern part of the study area. The changes were found mainly in the saturation zone. This is most likely due to the relative kinetic stabilization of the solutions infiltrating into the ground, once the saturation was reached.

In order to compare the mechanical properties of the primary zone (zone of natural soil condition) and the zone affected by the cementation process, 7 shallow DPL tests were performed in each zone. Text-fig. 9 presents the results of DPL tests. Dashed lines represent the primary zone – the ground out of the cementation zone, while solid lines represent ground under the cementation zone. Additionally, bold lines show the average penetration resistance for both zones separately.

SEM pictures of sand were taken with a scanning electron microscope coupled to an EDS microprobe, in order to identify the cementing substance. The samples showed the presence of quartz grains, feldspars, carbonates (calcite), gypsum, clay minerals, and a characteristic binder in the form of fibrous microcrystals (Text-fig. 10).

EDS microprobe analyses did not give unambiguous results on the mineral composition of the fibrous crystals, therefore diffraction analysis was conducted (Text-fig. 11). XRD analyses performed on the raw samples also did not give an unambiguous answer regarding the mineral composition of the binder. The predominance of quartz grains in the composition of the tested samples made it impossible to identify the associated minerals, so it was decided to remove fractions bigger than 0.06 mm (the samples were mechanically sieved through a 0.06 mm sieve). In such prepared samples, quartz was found to be dominant and the presence of ettringite $Ca_6Al_2[(OH)_{12}(SO_4)_3]\cdot26H_2O$ was clearly demonstrated. Also, calcite, plagioclase, smectite, and potassium feldspars and illite and/or micas and gypsum were identified.
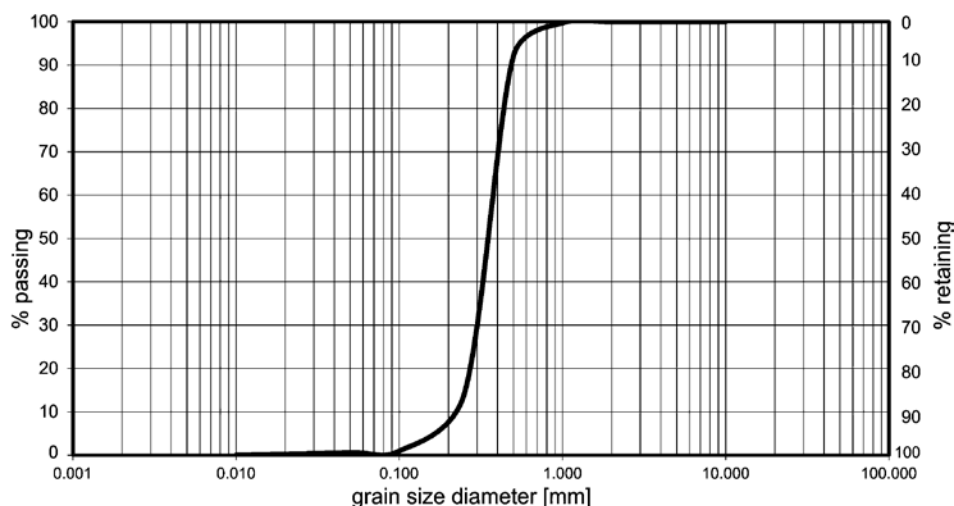
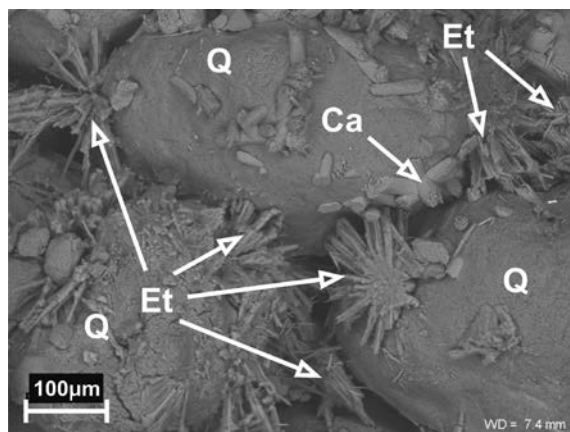Text-fig 8. Grain size distribution of cemented fluvial sand.
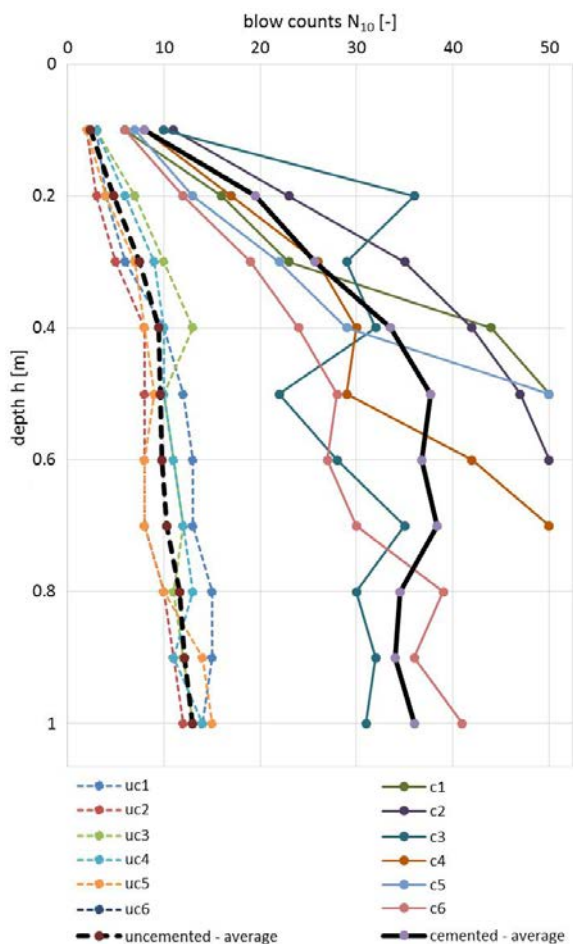
Text-fig. 9. DPL test results. Comparison of penetration resistance between uncemented fluvial sand (lines uc1–uc6) and cemented fluvial sand (lines c1–c6).

Text-fig. 10. Sample of cemented sand in SEM image. Q – quartz grain, Ca – calcite, Et – ettringite.
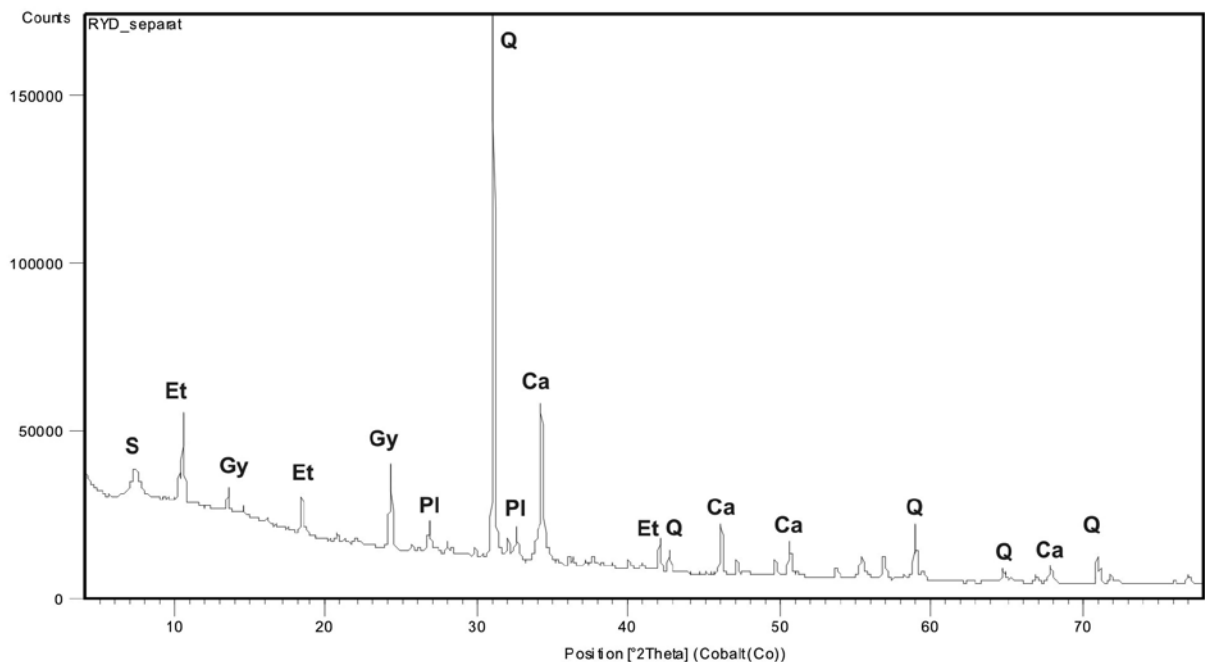
The $CaCO_3$ content determined by the Scheibler method was equal to 2.5%.

Chemical analysis of groundwater samples collected in the area (Text-fig. 1) showed SO_4^{2-} ion concentrations ranging from 56 to 105 mg/dm^3 (Table 1). The cation concentrations determined in the sample OW-0 (Text-fig. 1) are summarised in Table 2.

DISCUSSION

Chemical analyses of the components filling the pore spaces of fluvial sand identified ettringite as the main component of the cementing structures. The next stage of our investigation was to determine the origin of ettringite in the study area.

The crystal structure of ettringite has been described by Moore and Taylor (1970), among others. Ettringite is a hydrated calcium aluminosulphate: $Ca_6Al_2[(OH)_{12}(SO_4)_3] \cdot 26H_2O$. It occurs naturally in alkaline environments as a secondary mineral filling cracks in calcium-rich igneous rocks and metamorphic rocks (Hurlbut and Baum 1960; Murdoch and Chalmers 1960; Bentor *et al.*1963). Ettringite is also an important hydration product of Portland cements (Moore and Taylor 1970). It can be also formed by chemical reactions between active components of concrete and sulphate ions. During the cement manu-

Borehole number	Depth [m]	SO_4^{2-} [mg/dm3]	pH [-]
OW-0	4.0	98	8.05
OW-1	3.6	100	7.92
OW-2	3.8	95	7.86
OW-3	3.8	56	8.07
OW-4	4.0	59	8.11
OW-5	4.0	105	7.88

Table 1. Sulphate ion concentration (mg/dm^3) and pH of groundwater samples.

Al	Ba	Ca	Cd	Co	Cr	Cu	Fe	K
<0.000	0.005	133.253	<0.000	<0,000	<0.000	<0.000	<0.000	3.369
Mg	Mn	Na	Ni	Pb	Sr	Ti	V	Zn
11.202	<0.000	16.596	<0.000	<0.000	0.279	<0.000	<0.000	<0.000

Table 2. Cation concentration (mg/dm^3) in OW-0 sample.

Text-fig. 11. Diffractogram of the studied sample. Main reflections: Q – quartz, Et – ettringite, Ca – calcite, Gy – gypsum, Pl – plagioclase, S – smectite.

facturing process, a small amount of gypsum (ca. 3%) is usually added. Addition of a higher percentage of gypsum results in the formation of ettringite crystals in the slurry (Kurdowski 1991). Ettringite is a phase that forms very quickly in the cement slurry. Its content reaches a constant value after about 4 minutes and persists for about 6 hours, after which it increases relatively quickly to reach the maximum value after one day. Subsequently, the content of ettringite decreases gradually. However, a certain amount of ettringite can be found in concrete for a number of years (Mehta 1973; Taylor *et al.* 2001; Kurdowski and Szeląg 2011).

Literature data on the thermodynamic persistence of ettringite indicate that it is a very poorly soluble phase persistent over a wide temperature range (Mehta 1972; Brown and Bothe 1993; Warren and Reardon 1994; Constantiner and Farrington 1999).

There is lack of archival data on examples of natural concentrations of ettringite in late Pleistocene fluvial soil. However, a number of sources can be found describing ettringite in terms of construction activity and material testing of concrete and cement. Therefore, it can be assumed that the presence of ettringite in the studied sand is related to the historical engineering activity in the area.

While reconstructing the history of spatial devel-

opment of the area, we analysed aerial photographs from 1935 to 2020, available on the City of Warsaw website. at: https://mapa.um.warszawa.pl/mapaApp1/mapa?service=mapa_historyczna. We found a temporary concrete batching plant operating in the area most likely between 2007 and 2009 (Text-fig. 12).

The groundwater table is at a depth of about 3.5 m. The presence of cementation was noted in the upper parts of the saturation zone. During our exploratory drilling, structural strengthening (cementation) was found in the southeastern part of the analyzed area (in the AW-1 borehole), at a depth from 3.1 to 4.7 m below ground level. In the bottom of the excavation trench, the thickness of cemented sands was not less than 1 m. The elevation of the bottom of the excavation was close to the elevation of the groundwater table. The above observations indicate that cementation occurs at and below the groundwater table, and the cementation zone reaches a thickness of about 1.5–3.0 m. Contaminants infiltrated from the ground surface through the well-permeable aeration zone. When the groundwater level was reached, the flow of the solution stopped, the pressure gradient between the solution and the groundwater dropped to zero, and ettringite precipitation/crystallization occurred.

The entire thickness of the cemented zone was not drilled through with a hand auger during our field

Text-fig. 12. Aerial photograph of temporary concrete batching plant (on the left) in 2008, residential buildings (on the right) in 2019.

work. Information on the depth range of the structural changes was based on verbal communication from the contractor for the depression wells. The thickness of the cemented unit was estimated to average 2–3 m below the level of the excavation trench. Taking into account the horizontal extent (spread) of the cementation phenomenon, the volume of strengthened soil is about 6000 m^3.

The relatively large area affected by contamination is due to the absence of layers of poorly permeable soil (lack of natural insulation), as for example clayey silt (mud), which are often present in the river terraces. The absence of natural insulation in this area significantly helped the solution to migrate. Dissolution was very efficient, which was facilitated by the favorable grain size distribution of the sand, as it is well sorted medium sand, almost without fines (Text-fig. 8). These conditions probably encouraged the users of the concrete batching plant to dispose of liquid wastes directly to the groundwater environment.

According to the following reaction (Myneni *et al.* 1998; Perkins and Palmer 1999), the dissolution product of ettringite is sulphate ion:

$$Ca_6Al_2(SO_4)_3(OH)_{12} \cdot 26H_2O \rightarrow 6Ca^{2+} + 2Al^{3+} + 3SO_4^{2-} + 12OH^- + 26H_2O$$
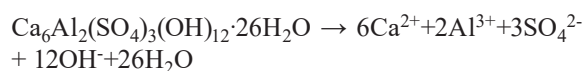
Despite the large variation in SO_4^{2-} ion concentrations in the groundwater samples, ranging from 56 to 100 mg/dm^3 (Table 2), the sulphate ion contents do not differ from the concentrations reported by other researchers within the Praga terrace (Mianowski

1997; Paczyński 1997; Porowska 2014). Sulphate concentrations do not exceed the drinking water standard (250 mg/dm^3). It should be noted, however, that the location of the boreholes was determined by the accessibility of the site. The residential development prevented borehole drillings in the SW part of the plot. The lack of ettringite effect on the higher sulfate content in groundwater is explained by its very poor solubility. The solubility (Ksp) of ettringite at ambient temperature reported in the literature ranges from 1.1×10^{-40} to 5.0×10^{-112} (Constantiner and Farrington 1999).

Cation concentrations (Table 2) also showed no anomalous values, including calcium (133.25 mg/dm^3) and aluminium (<0.000 mg/dm^3).

The DPL test results demonstrated a clear difference in terms of penetration resistance between the primary zone and the cemented zone. In the cementation zone, the blow count (N_{10}) is at least 3 times higher than in the primary zone (Text-fig. 9). Many times the penetration resistance exceeded 50 blow counts which resulted in stopping the test to avoid damaging the device. Thus, it could be assumed that in the deeper parts of the cemented zone strokes should be also higher than 50. Therefore, we assume that the penetration resistance of the cemented zone may be four, or even five times higher than that of the primary zone. The value of blow counts N_{10}, is expected to decrease to 11–15 below the cementation zone, which is an average value for fluvial sand at similar depth.

Comparison of DPL data (Text-fig. 9), revealed in a simplified way, the scale of the influence of uncontrolled strengthening of mechanical properties (deformability, stiffness) of fluvial sand. Direct determinations of strength and deformation characteristics require further studies.

CONCLUSIONS

The research conducted allowed us to identify the cause of the anomalies visible macroscopically in the bottom of the excavation. It was concluded that the observed change in colour and strengthening of soil structure is due to the activity of the temporary concrete batching plant, as indicated by the presence of ettringite – a component used in cement manufacturing. The estimated volume of strengthened sand is about 6 000 m^3 and the area affected by these changes is about 2500 m^2. When considering the effect of mechanical strengthening, it was found that the cementation zone covered by cementation showed at least three times higher penetration resistance than the zone without such changes.

Well sorted fluvial sand of high permeability is susceptible to anthropogenic transformations. Migration of liquid contaminants in such soil occurs easily and affects vast parts of the ground. The liquid contaminant concentrated mainly in the saturation zone, where the flow dynamics clearly weakened. The levelled bottom of the excavation showed spherical structures which were the result of the contamination wave movement.

Despite the release of contaminated solutions directly into the ground, currently there are no negative effects on groundwater, which is related to the very poor solubility of ettringite.

Acknowledgments

REFERENCES

ASTM D2487-17. Standard Practice for Classification of Soils for Engineering Purposes (Unified Soil Classification System). www.astm.org.

Bażyński, J., Drągowski, A., Frankowski, Z., Kaczyński, R., Rybicki, S. and Wysokiński, L. 1999. Principles of preparing engineering geological documentation. 184 pp. Polish Geological Institute; Warsaw. [In Polish]

Bentor, Y., Gross, S. and Heller, L. 1963. High-temperature minerals in non-metamorphosed sediments in Israel. *Nature*, **199** (4892), 478–479.

Brown, P.W. and Bothe Jr, J.V. 1993. The stability of ettringite. *Advances in Cement Research*, **5** (18), 47–63.

BS EN ISO 10693:2014. Soil quality. Determination of carbonate content. Volumetric method. www.en-standard.eu.

Constantiner, D. and Farrington, S.A. 1999. Review of the thermodynamic stability of ettringite. *Cement, concrete and aggregates*, **21** (1), 39–42.

Culshaw, M.G. and Price, S.J. 2011. The 2010 Hans Cloos lecture: the contribution of urban geology to the development, regeneration and conservation of cities. *Bulletin of Engineering Geology and Environment*, **70** (3), 333–376.

Dobak, P. and Chylińska, A. 2007. Dynamics of settlements changes caused by dewatering system in surroundings of the "Bełchatów" lignite mine, *Geologos*, **11**, 357–364. [In Polish]

Head, K.H. 1992. Manual of soil laboratory testing, Volume.1: Soil classification and compaction. 2nd ed. 388 pp. Pentech Presss; London.

Hurlbut Jr, C.S. and Baum, J.L. 1960. Ettringite from Franklin, New Jersey. American Mineralogist: *Journal of Earth and Planetary Materials*, **45** (11–12), 1137–1143.

Kong, T.B. and Komoo, I. 1990. Urban geology: case study of Kuala Lumpur, Malaysia. *Engineering Geology*, **28** (1–2), 71–94.

ISO 14688-2:2017. Identification and classification of soil. www.iso.org.

ISO 22476-2:2005. Geotechnical investigation and testing. www.iso.org.

Kowalczyk, S., Cabalski, K. and Radzikowski, M. 2017. Application of geophysical methods in the evaluation of anthropogenic transformation of the ground: A case study of the Warsaw environs, Poland. *Engineering Geology*, **216**, 42–55.

Kumor, M.K. 2016. Expansive clays of the subsoil in Bydgoszcz. Selected geotechnical problems. 233 pp. Wydawnictwo UTP; Bydgoszcz.

Kurdowski, W. 1991. Chemistry of concrete, 475 pp. Wydawnictwa Naukowe PWN; Warszawa. [In Polish]

Kurdowski, W. and Szeląg, H. 2011. Concrete destruction caused by delayed ettringite formation. *Infrastruktura Transportu*, **4**, 1119–1126. [In Polish]

Mehta, P.K. 1972. Stability of ettringite on heating. *Journal of the American Ceramic Society*, **55** (1), 55–57.

Mehta, P.K. 1973. Mechanism of expansion associated with ettringite formation. *Cement and concrete research*, **3** (1), 1–6.

Mianowski, Z. 1997. Hydrogeological Map of Poland in scale

1:50 000 with explanations, Piaseczno sheet, PIG-PIB; Warszawa. [In Polish]

Moore, A.E. and Taylor, H.F.W. 1970. Crystal structure of ettringite. *Acta Crystallographica Section B: Structural Crystallography and Crystal Chemistry*, **26** (4), 386–393.

Murdoch, J. and Chalmers, R.A. 1960. Ettringite ("Woodfordite") from Crestmore, California. *American Mineralogist*, **45** (11–12), 1275–1278.

Myneni, S.C., Traina, S.J. and Logan, T.J. 1998. Ettringite solubility and geochemistry of the $Ca(OH)_2$-$Al_2(SO_4)_3$-H_2O system at 1 atm pressure and 298 K. *Chemical Geology*, **148** (1–2), 1–19.

Paczyński, B. 1997. Hydrogeological Map of Poland in scale 1:50 000 with explanations, Warszawa Wschód sheet. PIG-PIB; Warszawa. [In Polish]

Pazdro, Z. and Kozerski, B. 1990. Hydrogeology, 624 pp. Wydawnictwa Geologiczne; Warszawa. [In Polish]

Perkins, R.B. and Palmer, C.D. 1999. Solubility of ettringite $(Ca_6[Al(OH)_6]_2(SO_4)_3 \cdot 26H_2O)$ at 5–75° C. *Geochimica et Cosmochimica Acta*, **63** (13–14), 1969–1980.

Porowska, D. 2014. Sulphur compounds in biogas and groundwater around the reclaimed municipal landfill in Otwock. *Przegląd Geologiczny*, **62** (11), 761–767. [In Polish]

Radzikowski, M., Cabalski, K. and Kowalczyk, S. 2017. Urban geology – A case study of Warsaw agglomeration. *Przegląd Geologiczny*, **65** (10/2), 883–889. [In Polish]

Sarnacka, Z. 1992. Stratigraphy of Quaternary sediments of Warsaw and its vicinity. Prace PIG – Tom 138, 27 pp. [In Polish]

Tang, H., Wasowski, J. and Juang, C.H. 2019. Geohazards in the three Gorges Reservoir Area, China – Lessons learned from decades of research. *Engineering Geology*, **261**, 1–16.

Taylor, H.F.W., Famy, C. and Scrivener, K.L. 2001. Delayed ettringite formation. *Cement and concrete research*, **31** (5), 683–693.

Warren, C.J. and Reardon, E.J. 1994 The solubility of ettringite at 25°C. *Cement and Concrete Research*, **24** (8), 1515–1524.